Biochimica et Biophysica Acta 1838 (2014) 1719–1729

Contents lists available at ScienceDirect

Biochimica et Biophysica Acta

journal homepage: www.elsevier.com/locate/bbamem

Functional mapping and implications of substrate specificity of the yeast high-affinity leucine permease Bap2

Yuki Usami [a,1], Satsohi Uemura [a,1], Takahiro Mochizuki [a], Asami Morita [a], Fumi Shishido [b], Jin-ichi Inokuchi [b], Fumiyoshi Abe [a,c,*]

[a] Department of Chemistry and Biological Science, College of Science and Engineering, Aoyama Gakuin University, Sagamihara, Japan
[b] Division of Glycopathology, Institute of Molecular Biomembrane and Glycobiology, Tohoku Pharmaceutical University, Sendai, Japan
[c] Institute of Biogeosciences, Japan Agency for Marine-Earth Science and Technology (JAMSTEC), Yokosuka, Japan

ARTICLE INFO

Article history:
Received 31 January 2014
Received in revised form 21 March 2014
Accepted 25 March 2014
Available online 31 March 2014

Keywords:
Saccharomyces cerevisiae
Leucine permease Bap2
Homology modeling
*log*P

ABSTRACT

Leucine is a major amino acid in nutrients and proteins and is also an important precursor of higher alcohols during brewing. In *Saccharomyces cerevisiae*, leucine uptake is mediated by multiple amino acid permeases, including the high-affinity leucine permease Bap2. Although *BAP2* transcription has been extensively analyzed, the mechanisms by which a substrate is recognized and moves through the permease remain unknown. Recently, we determined 15 amino acid residues required for Tat2-mediated tryptophan import. Here we introduced homologous mutations into Bap2 amino acid residues and showed that 7 residues played a role in leucine import. Residues I109/G110/T111 and E305 were located within the putative α-helix break in TMD1 and TMD6, respectively, according to the structurally homologous *Escherichia coli* arginine/agmatine antiporter AdiC. Upon leucine binding, these α-helix breaks were assumed to mediate a conformational transition in Bap2 from an outward-open to a substrate-binding occluded state. Residues Y336 (TMD7) and Y181 (TMD3) were located near I109 and E305, respectively. Bap2-mediated leucine import was inhibited by some amino acids according to the following order of severity: phenylalanine, leucine > isoleucine > methionine, tyrosine > valine > tryptophan; histidine and asparagine had no effect. Moreover, this order of severity clearly coincided with the log*P* values (octanol–water partition coefficients) of all amino acids except tryptophan. This result suggests that the substrate partition efficiency to the buried Bap2 binding pocket is the primary determinant of substrate specificity rather than structural amino acid side chain recognition.

1. Introduction

Leucine is a major amino acid in nutrients and proteins and is believed to account for approximately 20% of our protein intake [1]. Hence, organisms would be expected to have developed subtle mechanisms of leucine uptake and synthesis to fulfill the high demand for protein synthesis. Branched-chain amino acids including leucine, isoleucine, and valine are highly important in brewing because they are precursors of the higher alcohols, which in many cases, determine the flavors of alcoholic beverages. In *Saccharomyces cerevisiae*, these amino acids can be imported by multiple amino acid permeases, including the general amino acid permease Gap1 [2], the branched-chain amino acid permeases Bap2 [3] and Bap3 [4], the tryptophan/tyrosine permease Tat1 [5], the low-affinity amino acid permease Agp1 [6], and the high-affinity glutamine permease Gnp1 [7]. Gap1 is active on poor nitrogen sources such as proline, urea, or citrulline but is downregulated by ubiquitination on rich nitrogen sources such as ammonium ions, glutamine, or asparagine [8]. Eventually, under brewing conditions, amino acid permeases other than Gap1, most probably Bap2, Bap3, and Tat1, are thought to be the main contributors to branched-chain amino acid uptake. Bap2 is known as a high-affinity leucine permease; Bap3 is the closest homolog of Bap2 and is believed to have arisen from whole genome duplication [9]. Transcription of *BAP2* and *BAP3* is induced by amino acids such as leucine or phenylalanine and is under the control of the external amino acid-sensing plasma membrane Ssy1–Ptr3–Ssy5 complex [10]. Constitutive *BAP2* expression in a brewing yeast strain accelerates the assimilation of branched-chain amino acids during the brewing process. Bap2 is also regulated by ubiquitination at the posttranslational level; specifically, it undergoes Rsp5-dependent ubiquitination at its *N*-terminal lysine residues and subsequent endocytosis, followed by vacuolar degradation [11,12]. Therefore, subtle mechanisms regulate the cellular Bap2 level to control the branched-chain amino acid uptake in response to different external nitrogen source qualities.

Reportedly, commonly used laboratory strains such as BY4741 or W303 exhibited growth sensitivity to a synthetic complete (SC)

* Corresponding author at: 5-10-1 Fuchinobe, Chuo-ku, Sagamihara 252-5258, Japan. Tel.: +81 42 759 6233; fax: +81 42 759 6511.
E-mail address: abef@chem.aoyama.ac.jp (F. Abe).
[1] These authors contributed equally.

http://dx.doi.org/10.1016/j.bbamem.2014.03.018
0005-2736/

medium that contained high concentrations of non-essential amino acids [13]. The growth sensitivity was due to compromised leucine uptake in leucine auxotrophic strains; leucine likely competed with other amino acids, most probably isoleucine and valine, for Bap2 uptake. Strains carrying *leu2* are more sensitive than *LEU2* strains to acetic acid, a yeast fermentation by-product. At a concentration of 80 mM acetic acid at pH 4.8, leucine, lysine, histidine, tryptophan, phosphate, and glucose uptake were decreased to 5%–50% of that observed in cells in the absence of acetic acid [14]. Whether a particular auxotrophy caused acetic acid-mediated growth inhibition seemed to depend largely but not solely on the implicated amino acids. Although the regulatory mechanisms of *BAP2* transcription and the physiological importance of leucine availability have been extensively investigated, substrate specificity and the structure and mechanisms of Bap2-mediated leucine import remain unclear.

Crystallographic information regarding homologous proteins has provided us with clues about the mechanical properties of substrate import through structurally unknown permeases. Using random mutagenesis in combination with site-directed mutagenesis based on crystallographic studies of the *Escherichia coli* arginine/agmatine antiporter AdiC [15,16], we recently identified 15 amino acid residues in the Tat2 transmembrane domains (TMDs) 1, −3, −5–8, and −10 that were required for tryptophan import [17]. Residues T98, Y167, and E286 were assumed to form the central cavity of Tat2. G97/T98 and E286 were located within the putative α-helix break in TMD1 and TMD6, respectively, which are highly conserved among yeast amino acid permeases and bacterial solute transporters. Given the pronounced similarity between Bap2 and Tat2, with an identity of 39%, these permeases are expected to share mechanistic principles with regard to substrate import. Hence, we created homologous mutations into Bap2 to elucidate the required amino acid residues for leucine import. This comparative study on multiple permeases offers clues about the mechanisms of substrate recognition mediated by amino and carboxyl groups or specific side chains. In this study, we determined that 7 amino acid residues in the TMDs were required for Bap2-mediated high-affinity leucine import. We also proposed the hypothesis that Bap2 substrate selectivity is governed by the log*P* (octanol–water partition coefficient) of free amino acids.

2. Materials and methods

2.1. Yeast strains and culture conditions

The parental wild-type strain BY4741 (*MAT***a** *his3*Δ0 *leu2*Δ0 *met15*Δ0 *ura3*Δ0) and the deletion mutant *bap2*Δ::*KanMX* on the BY4741 genetic background were used in this study [18]. Unless otherwise specified, the cells were grown at 25 °C with shaking in synthetic complete (SC) medium, with slight modifications. The amino acid concentrations were as follows: 40 or 100 $\mu g \cdot mL^{-1}$ leucine, 30 $\mu g \cdot mL^{-1}$ isoleucine, 150 $\mu g \cdot mL^{-1}$ valine, 40 $\mu g \cdot mL^{-1}$ tryptophan, 20 $\mu g \cdot mL^{-1}$ histidine, 30 $\mu g \cdot mL^{-1}$ lysine, 20 $\mu g \cdot mL^{-1}$ methionine, 50 $\mu g \cdot mL^{-1}$ phenylalanine, 30 $\mu g \cdot mL^{-1}$ tyrosine, 20 $\mu g \cdot mL^{-1}$ arginine, 100 $\mu g \cdot mL^{-1}$ aspartic acid, 100 $\mu g \cdot mL^{-1}$ glutamic acid, 400 $\mu g \cdot mL^{-1}$ serine, and 200 $\mu g \cdot mL^{-1}$ threonine. Hereafter, SC 40Leu and SC 100Leu denote SC medium containing 40 and 100 $\mu g \cdot mL^{-1}$ leucine, respectively. In our analysis, an OD_{600} of 1 is comparable to 1.65×10^7 cells mL^{-1}.

2.2. Plasmid construction

The plasmids used in this study are listed in Table 1. pAK162 (p*TDH3*-3HA in pRS316 [19], [*CEN4 URA3*], a kind gift from Akio Kihara of Hokkaido University) was used to create the *BAP2* plasmid. First, the *BAP2* open-reading frame (ORF), along with its own promoter (p*BAP2*, 840-bp upstream of the ORF) and terminator (t*BAP2*, 440-bp downstream of the ORF) regions, was amplified from strain BY4741 genomic DNA, using the primers AACAGTCGACTCGGGCTTTCGTTGCCACTC and ATAGGGTACCTTCATGATGGCCTCCTAGTC. The resulting DNA fragment was cloned into the pGEM-T Easy vector (Promega, Madison, WI, USA) to yield pYU1. A DNA fragment containing the *BAP2* ORF with t*BAP2* alone was amplified using the primers ACTAGTATGCTATCTTCAGAAG ATTTTGGATCTTCTGG and ATAGGGTACCTTCATGATGGCCTCCTAGTC

Table 1
Plasmids used in this study.

Plasmid	Description	Source or reference
pRS316	*URA3 CEN*	[19]
pAK162	3HA, *URA3 CEN*	Provided by A. Kihara
pUA99	GFP, *URA3 CEN*	This study
pYU65	3HA-*BAP2* driven by *BAP2* promoter in pRS316	This study
pAM14	3HA-*BAP2* I109T driven by *BAP2* promoter in pRS316	This study
pAM15	3HA-*BAP2* G110V driven by *BAP2* promoter in pRS316	This study
pAM16	3HA-*BAP2* T111A driven by *BAP2* promoter in pRS316	This study
pAM17	3HA-*BAP2* L113S driven by *BAP2* promoter in pRS316	This study
pAM18	3HA-*BAP2* Y181L driven by *BAP2* promoter in pRS316	This study
pAM19	3HA-*BAP2* C182A driven by *BAP2* promoter in pRS316	This study
pYU58	3HA-*BAP2* K242R driven by *BAP2* promoter in pRS316	This study
pYU59	3HA-*BAP2* E305D driven by *BAP2* promoter in pRS316	This study
pYU66	3HA-*BAP2* Y336L driven by *BAP2* promoter in pRS316	This study
pYU61	3HA-*BAP2* I341L driven by *BAP2* promoter in pRS316	This study
pYU62	3HA-*BAP2* I343L driven by *BAP2* promoter in pRS316	This study
pYU63	3HA-*BAP2* F345L driven by *BAP2* promoter in pRS316	This study
pYU64	3HA-*BAP2* V347L driven by *BAP2* promoter in pRS316	This study
pAM12	3HA-*BAP2* S393G driven by *BAP2* promoter in pRS316	This study
pAM20	3HA-*BAP2* V394A driven by *BAP2* promoter in pRS316	This study
pAM21	3HA-*BAP2* W496L driven by *BAP2* promoter in pRS316	This study
pAM22	3HA-*BAP2* T470A driven by *BAP2* promoter in pRS316	This study
pUA196	3HA-*BAP2*-GFP driven by *BAP2* promoter in pRS316	This study
pUA197	3HA-*BAP2*-GFP I109T driven by *BAP2* promoter in pRS316	This study
pUA198	3HA-*BAP2*-GFP G110V driven by *BAP2* promoter in pRS316	This study
pUA199	3HA-*BAP2*-GFP T111A driven by *BAP2* promoter in pRS316	This study
pUA200	3HA-*BAP2*-GFP Y181L driven by *BAP2* promoter in pRS316	This study
pUA201	3HA-*BAP2*-GFP E305D driven by *BAP2* promoter in pRS316	This study
pUA202	3HA-*BAP2*-GFP Y336L driven by *BAP2* promoter in pRS316	This study
pUA203	3HA-*BAP2*-GFP V394A driven by *BAP2* promoter in pRS316	This study

and pYU1 as the template DNA. The resulting DNA fragment was cloned into the pGEM-T Easy vector to yield pYU134. The p*TDH3* of pAK162 was replaced with p*BAP2*, which was generated using the primers CGGGCCCCCCCTCGAGGGGCTTTCGTTGCCACTCTTCAGGAT and ACTCAT GGTTCCCCCGGGGAGTTTTATTGAAGCTAAATAAATTGATAGTATCG from pYU1 as a template, to yield pUA134. Finally, the *Spe*I-digested DNA fragment from pYU13 was introduced into pUA135 to yield pYU65 (p*BAP2*-3HA-*BAP2*-t*BAP2* [*CEN4 URA3*]), which was used for Western blot analyses.

To generate a *BAP2*-GFP plasmid, the p*BAP2*-3HA-*BAP2* region was amplified using the primers CTCACCATGGTGCCCGGGCACCAGAAATGA TAAGCTTTTCTCATCAA and TGCTCACCATGGATCCACACCAGAAATGAT AAGCTTTTCTCATC and pYU65 as a template. The resulting DNA fragment was introduced into pUA99 (EGFP-t*TDH3*, *CEN4 URA3*) to yield pUA196 (p*BAP2*-3HA-*BAP2*-EGFP-t*TDH3* [*CEN4 URA3*]), which was used for fluorescence microscopic analyses.

PCR-based site-directed mutagenesis was performed to create amino acid substitutions in the Bap2 TMDs, using PrimerSTAR Max (TaKaRa Bio Inc., Otsu, Shiga, Japan), relevant primers, and pYU65 as a template. The appropriate base substitution was confirmed by sequencing the *BAP2* ORF with the relevant sequence primers. The resulting 3HA-*BAP2* ORFs were introduced into pUA99 to yield the mutant forms of the 3HA-*BAP2*-GFP plasmids.

2.3. Western blotting

Whole cell extract preparation was performed as described previously, with a slight modification [20]. In brief, 10^8 cells in the exponential growth phase ($1.0–1.5 \times 10^7$ cells·mL^{-1}) were collected by centrifugation, washed serially with 10 mM NaN_3–10 mM NaF and lysis buffer A (50 mM Tris–HCl, 5 mM EDTA, 10 mM NaN_3, 1 mM PMSF, and 1 Complete™ EDTA-free tablet [Roche, Mannheim, Germany] for 50 mL, pH 7.5), and disrupted with glass beads at 4 °C. Unbroken cells and debris were removed by centrifugation at 900 ×*g* for 5 min, and the cleared lysates were treated with 5% SDS–5% 2-mercaptoethanol at 37 °C for 10 min to denature the proteins. To obtain the P13 membrane fraction, the whole cell extracts were subjected to centrifugation at 13,000 ×*g* for 10 min, and the resulting pellets were treated with 5% SDS–5% 2-mercaptoethanol at 37 °C for 10 min. Antibodies against hemagglutinin (HA; InvivoGen, San Diego, CA, USA), Pma1 (40B7, Abcam, Cambridge, UK), Pep12 (2C3G4, Abcam), and Dpm1 (5C5A7, Life Technologies Corp., Carlsbad, CA, USA) were used. Adh1 and Pma1 were used as loading controls for the whole cell extracts and the P13 membranes, respectively. Dpm1 was used as a loading control for both the P13 and P100 membranes. The signals were detected with an ImageQuant LAS4000 mini (GE Healthcare Life Sciences, Piscataway, NJ, USA).

2.4. Subcellular fractionation

Cells were fractionated using differential centrifugation, as described previously [20]. Whole-cell lysates, prepared as described above, were subjected to centrifugation at 13,000 ×*g* for 10 min to yield a P13 (pellet) fraction. The resulting supernatant fraction was subjected to centrifugation at 100,000 ×*g* for 30 min to yield a P100 (pellet) fraction. The cells were also fractionated by centrifugation on a sucrose density gradient to separate the cellular membranes. The cells were washed twice with 10 mM NaN_3, once with 10 mM Tris–HCl (pH 7.5)–10 mM NaN_3, and once with 100 mM Tris–HCl (pH 9.4)–40 mM 2-mercaptoethanol. The cells were then resuspended in 50 mM Tris–HCl (pH 7.5)–1.2 M sorbitol and treated with 2 mg·mL^{-1} of zymolyase 100 T for 30 min at 30 °C to obtain spheroplasts. The spheroplasts were collected by centrifugation and were homogenized with a 27-gauge needle 6 times. After removing the unbroken cells by centrifugation, the cell lysate was placed on a sucrose density gradient (30, 45, 50, 55, and 60%) for centrifugation at 256,000 ×*g* for 5 h. Five fractions (each 840 μL) were collected from the top, and the proteins were treated with 5% SDS–5% 2-mercaptoethanol at 37 °C for 10 min to denature the proteins.

2.5. Leucine import assay

L-[4, 5-^{3}H] leucine (MT-672E, 5.18 TBq·mmol^{-1}, 37 MBq·mL^{-1}, 1.01 μg·mL^{-1}; Moravek Biochemicals, Inc., Brea, CA, USA) was used for the leucine import assay. This assay was performed as described previously, with some modifications [17,21]. The cells were grown in SC 100Leu at 25 °C with shaking, washed twice, and resuspended in SC 40Leu medium, after which the cell culture was maintained for an additional 6 h. The cells were collected by centrifugation, washed twice with the assay buffer [50 mM 2-morpholinoethanesulfonic acid (Mes), 20 mM $(NH_4)_2SO_4$, 2% D-glucose, pH 5.0], and resuspended in the assay buffer with 4 μg·mL^{-1} leucine at a cell density of approximately 3×10^7 cells·mL^{-1}. ^{3}H-labeled leucine at a concentration of 1/1000 of the total volume was added to the cell suspension to begin the assay. A vacuum aspirator was used to trap 300 μL of cell suspension on pairwise-stacked GF/C glass filters, followed by a wash step with 20 mL of ice-cold distilled water. The quantity of incorporated leucine was then measured using a liquid scintillation counter. In our experimental conditions (4 μg·mL^{-1} = 30.5 μM leucine), 1 DPM for L-[4, 5-^{3}H] leucine could be converted to 10.4 fmol of incorporated non-labeled leucine in the cells. The data are expressed as the mean values of incorporated amino acid (pmol·10^7 cells^{-1} min^{-1}) and the standard deviations were obtained from 3 independent experiments.

2.6. Fluorescence microscopy

Cells expressing GFP-tagged Bap2 proteins were imaged using a fluorescence microscope (model IX70; Olympus, Co. Ltd., Tokyo, Japan).

2.7. Structural modeling

The ESyPred3D Web Server 1.0 software (http://www.fundp.ac.be/sciences/biologie/urbm/bioinfo/esypred/), an automated homology modeling program with increased alignment performances based on the modeling package MODELLER, was used [22,23]. The profile query for Bap2 yielded the *E. coli* arginine/agmatine antiporter AdiC (PDB entries: 3LRB and 3L1L) as a structural template [15,16]. An alignment was created for this template, and the Bap2 model was constructed using the PyMOL Molecular Graphics System, Version 1.5.0.4 Schrödinger, LLC (http://www.pymol.org/) [24].

3. Results

3.1. bap2Δ cells exhibit defective growth in SC 40Leu medium

Before functionally analyzing Bap2 mutants, it was necessary to establish an appropriate evaluation system. Because leucine could potentially be imported by multiple amino acid permeases, including Bap2, Bap3, Tat1, and Gap1, it was necessary to distinguish Bap2-mediated leucine import from the others. The *ssy1*Δ*gap1*Δ mutant was reported to be defective in leucine uptake and exhibit a growth deficiency similar to that of the *bap2*Δ*bap3*Δ*tat1*Δ*gap1*Δ mutant when grown on YPD medium, in which leucine, isoleucine, and valine synthesis was inhibited by metsulphuron methyl [10]. For the following reasons, however, we did not employ the *ssy1*Δ*gap1*Δ mutant to evaluate Bap2 function in this study. First, the *ssy1*Δ*gap1*Δ mutant was defective in the uptake of several amino acids, including tyrosine, glutamate, tryptophan, serine, and methionine, in addition to the branched-chain amino acids [10]. Second, the *ssy1*Δ mutation is synthetic-lethal when combined with the *leu2* mutation, which is an auxotrophic marker of the wild-type strain BY4741 [25]. Instead, we sought to determine the critical leucine concentration in SC medium at which only the *bap2*Δ mutant exhibited growth defects. This would allow us

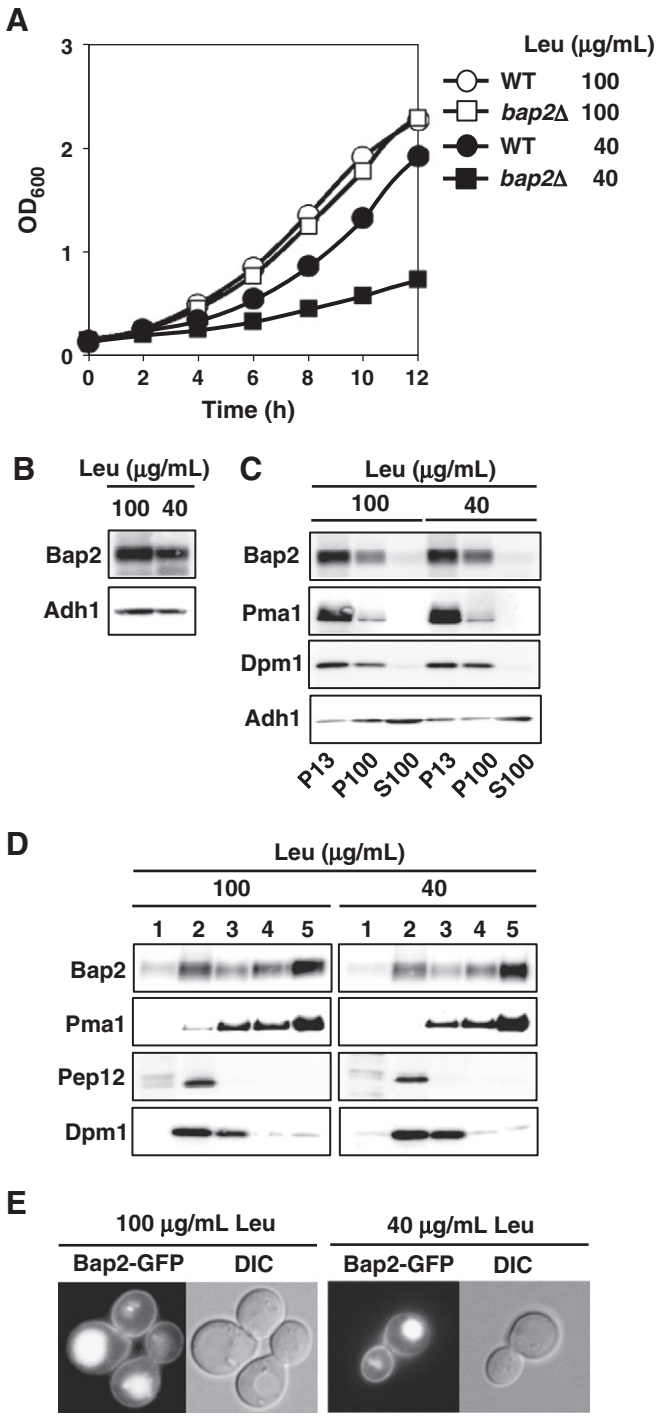

Fig. 1. Cell growth and Bap2 protein expression under high and low leucine concentrations. (A) Cell growth of the wild type (*bap2*Δ cells harboring a 3HA-*BAP2* plasmid) and *bap2*Δ mutant strains (*bap2*Δ cells harboring an empty vector alone) in SC 100Leu or SC 40Leu medium. (B) Whole cell extracts from the wild type strain were subjected to Western blot analysis to detect 3HA-Bap2 proteins. Whole cell extracts from the wild type strain were subjected to differential centrifugation (C) or centrifugation on a sucrose density gradient (D) to separate the membranes, followed by Western blot analysis. (E) Visualization of Bap2-GFP proteins via fluorescence microscopy. Adh1, Pma1, Dpm1, and Pep12 were used as marker proteins for the cytoplasm, plasma membrane, ER, and endosomes, respectively.

to evaluate Bap2 mutations under more physiologically natural conditions. While both the wild-type and *bap2*Δ strains grew equivalently at a high leucine concentration (100 $\mu g \cdot mL^{-1}$), the *bap2*Δ cells exhibited a slow growth phenotype at a low leucine concentration (40 $\mu g \cdot mL^{-1}$) (Fig. 1A). However, both the wild-type and *bap2*Δ cells exhibited defective growth at a very low leucine concentration (4 $\mu g \cdot mL^{-1}$), likely because high isoleucine (30 $\mu g \cdot mL^{-1}$) and valine (150 $\mu g \cdot mL^{-1}$) concentrations in the SC medium competed for leucine uptake; additionally, 4 $\mu g \cdot mL^{-1}$ of leucine is an insufficient concentration to fulfill the high demand for leucine during protein synthesis (data not shown). Therefore, subsequent analyses were performed at 40 and 100 $\mu g \cdot mL^{-1}$ leucine in SC medium (SC 40Leu and SC 100Leu, respectively). Unless otherwise specified, we kept cell culture in SC 40Leu medium for 6 h. Hereafter, "wild type" denotes the *bap2*Δ mutant that carried 3HA-*BAP2* in a centromere-based plasmid, and "*bap2*Δ" denotes the *bap2*Δ mutant that carried an empty vector alone.

There were no marked differences in the Bap2 protein levels between the cells grown in SC 100Leu and SC 40Leu media (Fig. 1B). Whole cell extracts were subjected to differential centrifugation to yield the P13 membrane fraction in which the majority of the plasma membrane was retrieved, as well as the P100 membrane fraction in which half-quantities of the endosomes and ER membranes were retrieved. Bap2 proteins were discovered not only in the P13 fraction, but also to a lesser extent in the P100 fraction (Fig. 1C). There was little difference in Bap2 distribution between cells grown in SC 100Leu and those grown in SC 40Leu medium. We further subjected the whole cell extracts to sucrose density gradient centrifugation to precisely fractionate the internal membranes. We found that Bap2 co-localized with both the plasma membrane marker Pma1 and the endosomal marker Pep12, indicating that Bap2 is delivered to the cell surface and targeted to the vacuoles for degradation through the endocytic pathway (Fig. 1D). Few differences in Bap2 localization were observed in cells grown under different leucine concentrations. As a convenient Western blot analysis method, we used the P13 membranes to examine the levels of Bap2 mutant proteins, rather than isolating internal membranes on a sucrose density gradient. To validate the Bap2 distribution revealed by membrane fractionation, we confirmed the localization of Bap2-GFP to the plasma membrane and endosomes using fluorescence microscopy (Fig. 1E).

3.2. Rationale for mutation design

We have identified 15 amino acid residues that are required for Tat2-mediated tryptophan import by means of random mutagenesis and site-directed mutagenesis based on structural information about *E. coli* AdiC [15–17]. Given the pronounced similarity, we rationalized an examination of the Bap2 amino acid residues homologous to the 15 residues in Tat2. The amino acid sequences of the 5 permease proteins are aligned in Fig. 2 [26]. TMD1, −3, −6, −8, and −10 were found to be located interiorly in the overall folding structure of AdiC [15,16]. The AdiC substrate-binding motifs GSG (TMD1) and GVESA (TMD6) were conserved in both Tat2 (GTG and GIEMT, respectively) and Bap2 (GTG and GMELF, respectively). Therefore, I109T, G110V, T111A, L113S (TMD1), and E305D (TMD6) mutations were introduced into Bap2. In particular, E305, a fully conserved amino acid residue among yeast amino acid permeases, corresponds to E208 in AdiC, in which this residue plays a central role in arginine transport as the distal gate [15,16]. The central AdiC cavity comprises N22 and S26 from TMD1, Y93 from TMD3, E208 from TMD6, and Y365 from TMD10, which correspond to T107, T111 (TMD1), Y181 (TMD3), E305, and W469 (TMD10) in Bap2, respectively. Therefore, Y181L and W469L mutations were introduced into Bap2 along with T111A and E305D. K242 (TMD5) is also fully conserved among yeast amino acid permeases, and therefore a K242R mutation was introduced into Bap2. Gap1 is considered a transceptor, or a transporter protein with a receptor function. S388 and V389 are amino acid restudies of which the side chain was shown to protrude into the amino acid biding site of Gap1, and they were partially required for amino acid activation of PKA pathway signaling [27]. The corresponding sites in TMD8 were mutated in Bap2 to create S393G and V394A, respectively; these residues are not conserved in AdiC. In addition to these amino acid residues that were rationalized according

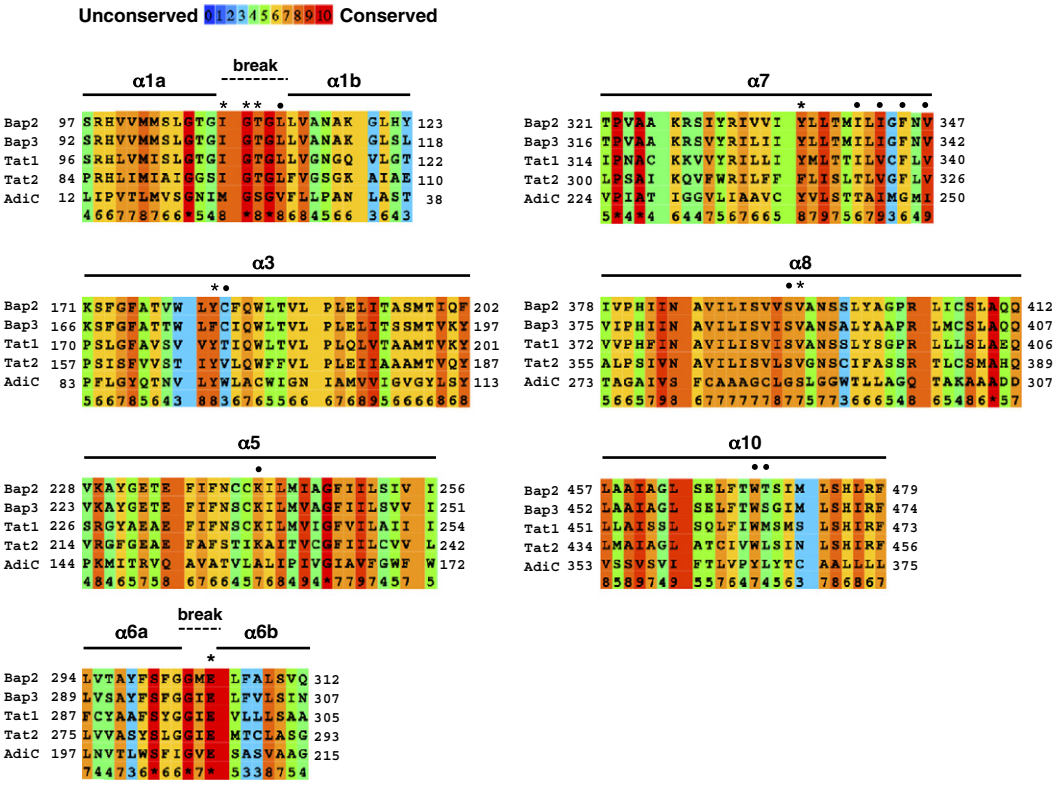

Fig. 2. Sequence alignments of TMD α-helices 1, −3, −5–8, and −10 in Bap2, Bap3, Tat1, Tat2, and *E. coli* AdiC. The residues mutated in this study are marked at the top. The alignments were constructed with the PRALINE multiple-sequence alignment program [26]. TMD α-helices were assigned according to the crystallographic structures of AdiC (PDB: 3L1L) [16]. TMDα1 and TMDα6 are divided by an α-helix break to yield TMDα1a/TMDα1b and TMDα6a/TMDα6b, respectively, according to the AdiC structure (PDB: 3L1L) [16]. Amino acid residues essential for Bap2-mediated leucine import are indicated by asterisks (*), and residues prone to mutation are indicated by dots (•). α denotes an α-helix. The numbers in the bottom rows indicate consistency scores derived from PRALINE.

to their roles in AdiC function, we introduced additional mutations in TMD3, TMD7, and TMD10, for which the significances were validated in Tat2 [17]. These were C182A (TMD3), Y336L, I341L, I343L, F345L, and V347L (TMD7). In total, 17 amino acid residues were individually mutated in Bap2 (Fig. 2 and Table 2).

3.3. Functional analysis of Bap2 mutant proteins

Cells growing exponentially in SC 100Leu medium were diluted in SC 100Leu or SC 40Leu medium to obtain 0.1 OD_{600} cell cultures (approximately 1.65×10^6 cells·mL^{-1}). The cells were cultured for

Table 2
Mutated amino acid residues in Bap2 and corresponding Tat2 and AdiC residues.

Bap2 mutation	TMD[1)]	Bap2 function[2)]	Corresponding Tat2 mutation	Tat2 function[3)]	Corresponding AdiC residue
I109T	1	−	I96T	−	M24
G110V	1	−	G97V	−	G25
T111A	1	−	T98A	−	S26
L113S	1	+	L100S	−	V28
Y181L	3	−	Y167L	−	Y93
C182A	3	+	V168A	−	W94
K242R	5	+	K228R	−	A158
E305D	6	−	E286D	−	E208
Y336L	7	−	F315L	−	Y239
I341L	7	+	T320L	−	T244
I343L	7	+	V322L	−	I246
F345L	7	+	F324L	−	G248
V347L	7	+	V326L	−	I250
S393G	8	+	S370G	−	G288
V394A	8	−	V371A	−	S289
W469L	10	+	W446L	+/−	Y365
T470A	10	+	L447S	+/−	L366

1) TMDs were assigned based on the crystallographic structure of AdiC (PDB: 3L1L).
2) Bap2 function was evaluated by the complementation test for growth in SC 40Leu medium.
−, no or poor growth; +, growth.
3) Tat2 function was evaluated by the complementation test for growth on SD 4Trp and YPD agar plates (Ref. [17]).
−, no growth; +/−, poor growth; +, growth.

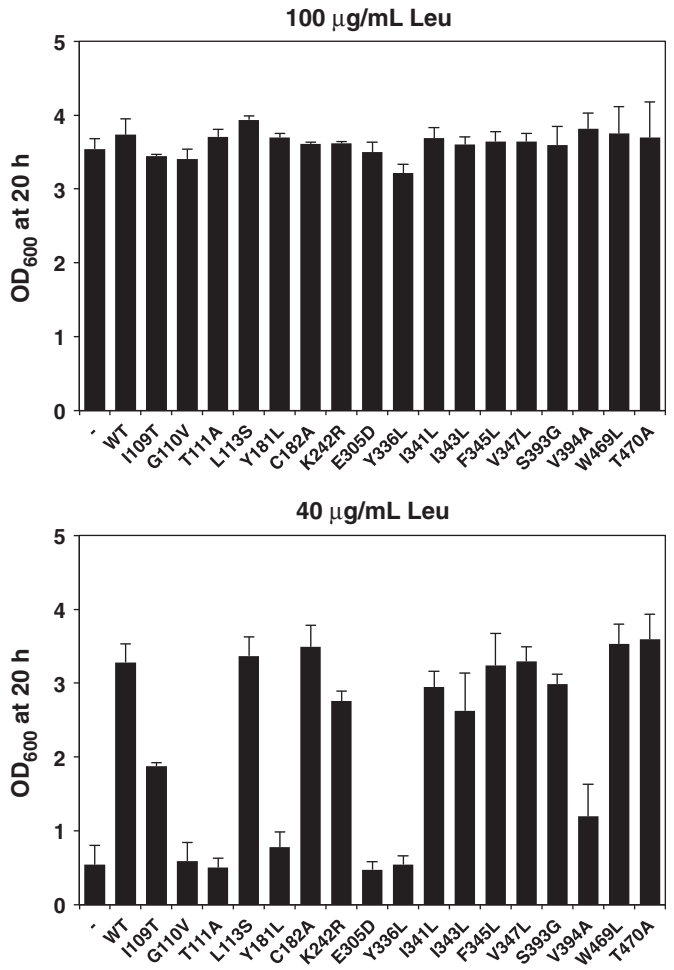

Fig. 3. Effects of Bap2 mutations on cell growth. Bap2 mutant proteins were expressed in *bap2*Δ cells. The cells were cultured in SC 100Leu or SC 40Leu medium for 20 h at 25 °C, beginning at an OD_{600} value of 0.1.

20 h at 25 °C, and the OD_{600} values were measured. There were no measureable differences in growth in SC 100Leu medium among these strains; however, mutant strains carrying I109T, G110V, T111A, Y181L, E305D, Y336L, or V394A single mutations in Bap2 exhibited significant growth defects in SC 40Leu medium (Fig. 3). These results suggested that the 7 amino acid residues were required for Bap2-mediated leucine import. This was in sharp contrast to the finding that 15 amino acid residues were required for Tat2-mediated tryptophan import.

To eliminate the possibility that any mutations diminished Bap2 synthesis and surface delivery, plasma membrane localization was confirmed in the 7 mutant proteins. Cells were grown in SC 100Leu or SC 40Leu medium, and P13 membrane fractions were prepared from whole cell extracts to enrich the plasma membrane concentrations. Despite some variations in the levels, Bap2 proteins in both the wild-type and mutant cells were almost equally localized in the P13 membranes (Fig. 4). To support this result, Bap2-GFP fusion proteins were expressed in *bap2*Δ cells and visualized using fluorescence microscopy. We confirmed that Bap2-GFP fusion proteins with I109T, T111A, Y181L, Y336L, E305D, and V394A mutations localized to the plasma membrane as well as did the wild type Bap2, thus justifying the growth analysis and subsequent leucine import assay. However, Bap2-GFP fusion proteins carrying G110V mutation accumulated in the ER rather than the plasma membrane (Fig. 5). Next, we noticed that GFP-fusion-Bap2^{G110V} or -Bap2^{E305D} expression led to a prolonged initiation of *bap2*Δ cell growth after the inoculation of cell aliquots from a SD agar plate into SC 100Leu medium, which also occurred with the 3HA-tagged mutant forms (data not shown). It is possible that the fused GFP caused Bap2 protein misfolding in the ER when combined with the G110V mutation, and G110V and E305D mutations might have exerted some stress on the cells at the onset of cell growth.

3.4. Leucine uptake by Bap2 and the relevance of logP to substrate recognition

Leucine uptake was measured using ^{3}H-labeled leucine. Initially, we attempted to use SC 40Leu medium to compare the import activities of the wild type and *bap2*Δ cells because the differences in their growth rates were clearly distinguishable (Fig. 1A). Unexpectedly, *bap2*Δ cells were able to import leucine as efficiently as the wild-type cells (data not shown). We attempt to explain this puzzling result as follows. In this assay, the cells were resuspended in fresh SC 40Leu medium that contained 40 $\mu g \cdot mL^{-1}$ leucine. This might have allowed the low-affinity leucine permeases Bap3 and/or Tat1 present in *bap2*Δ cells to import leucine. During the long-term incubation (more than several hours; Fig. 1A), the cells gradually consumed leucine, and consequently the leucine concentration decreased. In addition, the coexisting isoleucine and valine competed against leucine import. Under these conditions, only the high-affinity leucine permease Bap2 could contribute to leucine import to support cell growth. Eventually, the assay was performed with a buffer [50 mM 2-morpholinoethanesulfonic acid (Mes), 20 mM $(NH_4)_2SO_4$, 2% D-glucose, pH 5.0] that contained a low leucine

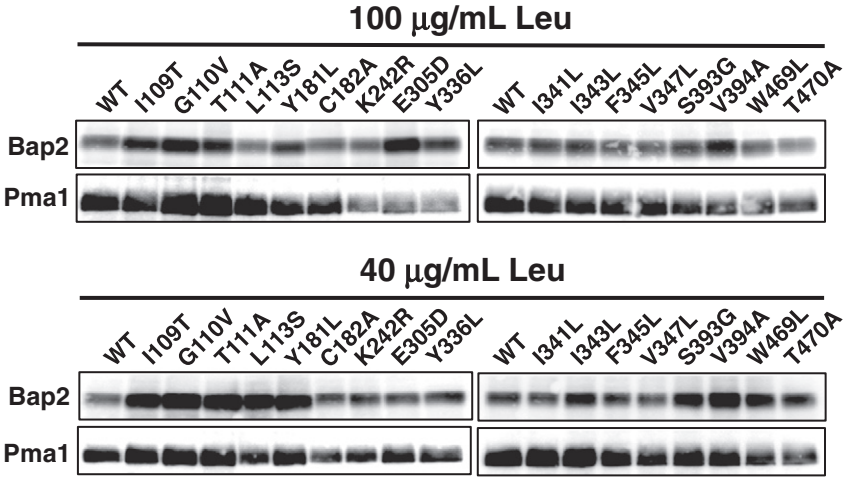

Fig. 4. Bap2 mutant protein expression. Bap2 mutant proteins were expressed in *bap2*Δ cells grown in SC 100Leu or SC 40Leu medium. The P13 membranes were collected by centrifugation at 13,000 ×*g* for 10 min. The membranes were subjected to Western blot analysis to detect 3HA-Bap2 and Pma1 with specific monoclonal antibodies.

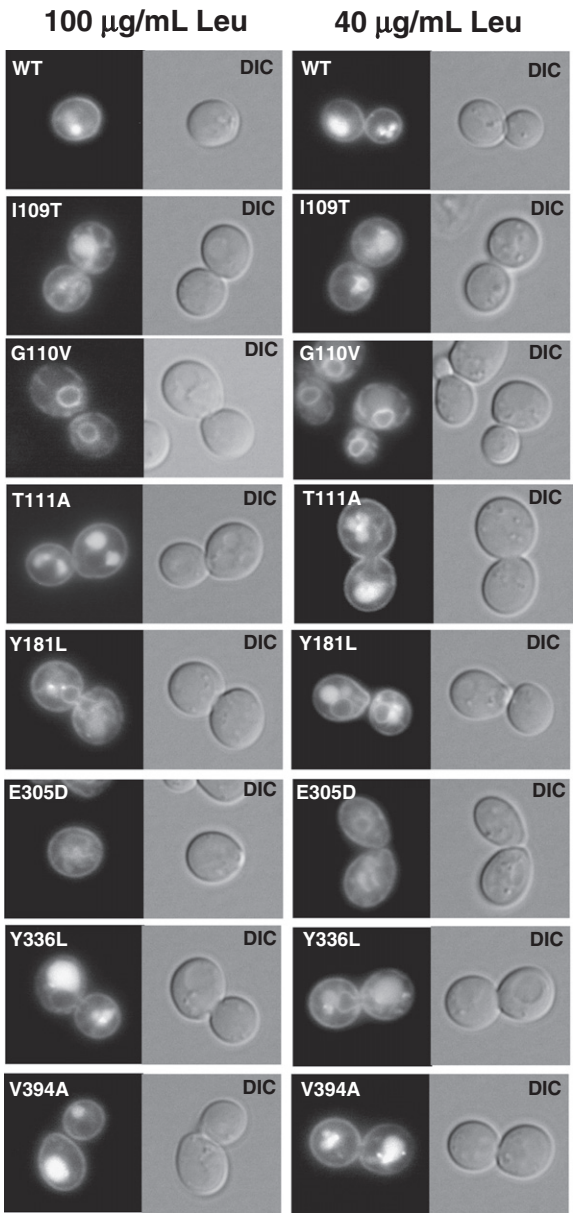

Fig. 5. Bap2 mutant protein localization. GFP-tagged Bap2 mutant proteins were expressed in *bap2*Δ cells. Exponentially growing cells in SC 100Leu or SC 40Leu medium were imaged via fluorescence microscopy.

concentration (4 μg·mL^{-1}) in the absence of isoleucine and valine, rather than SC 40Leu medium (see the Materials and methods section).

Cells were grown in either SC 100Leu or SC 40Leu medium, washed twice, and resuspended in the import assay buffer that contained a 1/1000 volume of ^{3}H-labeled leucine. The wild type cells imported leucine at a rate of approximately 30 pmol 10^{7}·cells min^{-1} when grown in either SC 100Leu or SC 40Leu medium (Fig. 6A). The *bap2*Δ cells exhibited reduced leucine import activity when grown in SC 100Leu medium and defective import activity when grown in SC 40Leu medium. This result suggested that leucine permeases other than Bap2 were downregulated during culture in SC 40Leu medium. Accordingly, the import assay could effectively evaluate Bap2 activity when SC 40Leu medium was used as the growth medium. The leucine uptake was time-dependent and exhibited a linear dependence on the incubation time for up to 10 min, and therefore all subsequent measurements were performed for 10 min (Fig. 6A).

To gain insight regarding substrate specificity, we measured Bap2-mediated leucine import (leucine 4 μg·mL^{-1} = 30.5 μM) in the presence of 10-fold higher concentrations (305 μM) of some non-radiolabeled amino acids. As shown in Fig. 6B, ^{3}H-labeled leucine import was strongly inhibited by leucine, isoleucine, and phenylalanine and moderately inhibited by methionine, tyrosine, valine, and tryptophan. In contrast, histidine and asparagine did not cause inhibition. The order of effect strength was phenylalanine, leucine > isoleucine > methionine, tyrosine > valine > tryptophan. This result suggested that leucine, isoleucine, and phenylalanine were preferred high-affinity substrates that competed for Bap2. This finding agreed with a previous finding that *BAP2* overexpression under the control of the *TPI1* promoter increased the uptake of phenylalanine, leucine, isoleucine, methionine, tyrosine, valine, and tryptophan but not histidine and arginine [28]. Next, we plotted the degree of inhibition versus the molecular weights, hydropathy indices that represent the hydrophobic or hydrophilic properties of the side chain [29], or log*P* values (octanol–water partition coefficient) of these amino acids (Data Book of Molecules; http://www.ecosci.jp/ec.html). We found that the degree of inhibition clearly correlated with the log*P* of all amino acids except tryptophan and represented a correlation coefficient of $R^2 = 0.957$ (Fig. 6C). Tryptophan deviated considerably from the correlation curve obtained with the other 8 amino acids. We assumed that the Bap2 substrate-binding site was hydrophobic and thereby would accommodate amino acid side chains with certain degrees of hydrophobicity and bulkiness. Importantly, the amino acid hydropathy index exhibited a rather low correlation with the degree of leucine import inhibition when compared with the log*P* (Fig. 6C). This led to a hypothesis in which the free amino acid partition efficiency to the buried binding pocket would be the primary determinant of the broad range of Bap2 substrate specificity, rather than the side chain property alone. Although it is speculative, our hypothesis would explain the reduced requirement for amino acid residues in Bap2-mediated leucine import, compared with that of Tat2-mediated import (see the Discussion section).

Seven Bap2 mutations were selected for the import assay according to the significance of the associated growth defects; these were I109T, G110V, T111A, Y181L, E305D, Y336L, and V394A. We found that these mutations compromised leucine import to various degrees in the following order of severity: G110V, T111A, E305D, Y336L > Y181L, V394A > > I109T (Fig. 7). The defective import severities agreed well with the growth abilities of the cells in SC 40Leu medium (Fig. 3).

3.5. Functional mapping of amino acid residues on the modeled Bap2 structures

Bap2 structure models were based on the *E. coli* AdiC outward-open (template, PDB 3LRB) [15] and occluded (template, PDB 3L1L) [16] structures, as previously performed for Tat2 [17]. Overall, the modeled Bap2 structures were similar to those of Tat2, except that the Bap2 TMD12 did not form an obvious α-helix structure (Fig. 8). There was a putative trajectory of leucine translocation within the Bap2 outward-open model. AdiC is known to undergo major conformational changes in TMD2, TMD6, and TMD10 upon arginine binding, resulting in the substrate-binding occluded conformation [16]. Correspondingly, structural conversion from the outward-open to the occluded structure was observed in Bap2. The 7 critical amino acid residues were mapped onto the Bap2 structural models (Fig. 8). I109, G110, and T111 (TMD1) were located within or adjacent to the GTG motif, which corresponds to the GSG motif of AdiC. The GSG motif of AdiC is located within the TMD1 helix-break region and fulfills a role in arginine carboxyl group recognition [16]. Hence, the significance of Bap2 I109, G110, and T111 is considered the recognition of the leucine carboxyl group. In Bap2, a contiguous L113S mutation had no effect on leucine import, whereas the corresponding L100S mutation diminished tryptophan import. T111, Y181 (TMD3), and E305 (TMD6) were assumed to form the central cavity of Bap2, and mutations in these amino acid residues abolished leucine import. The C182A mutation had no effect on leucine

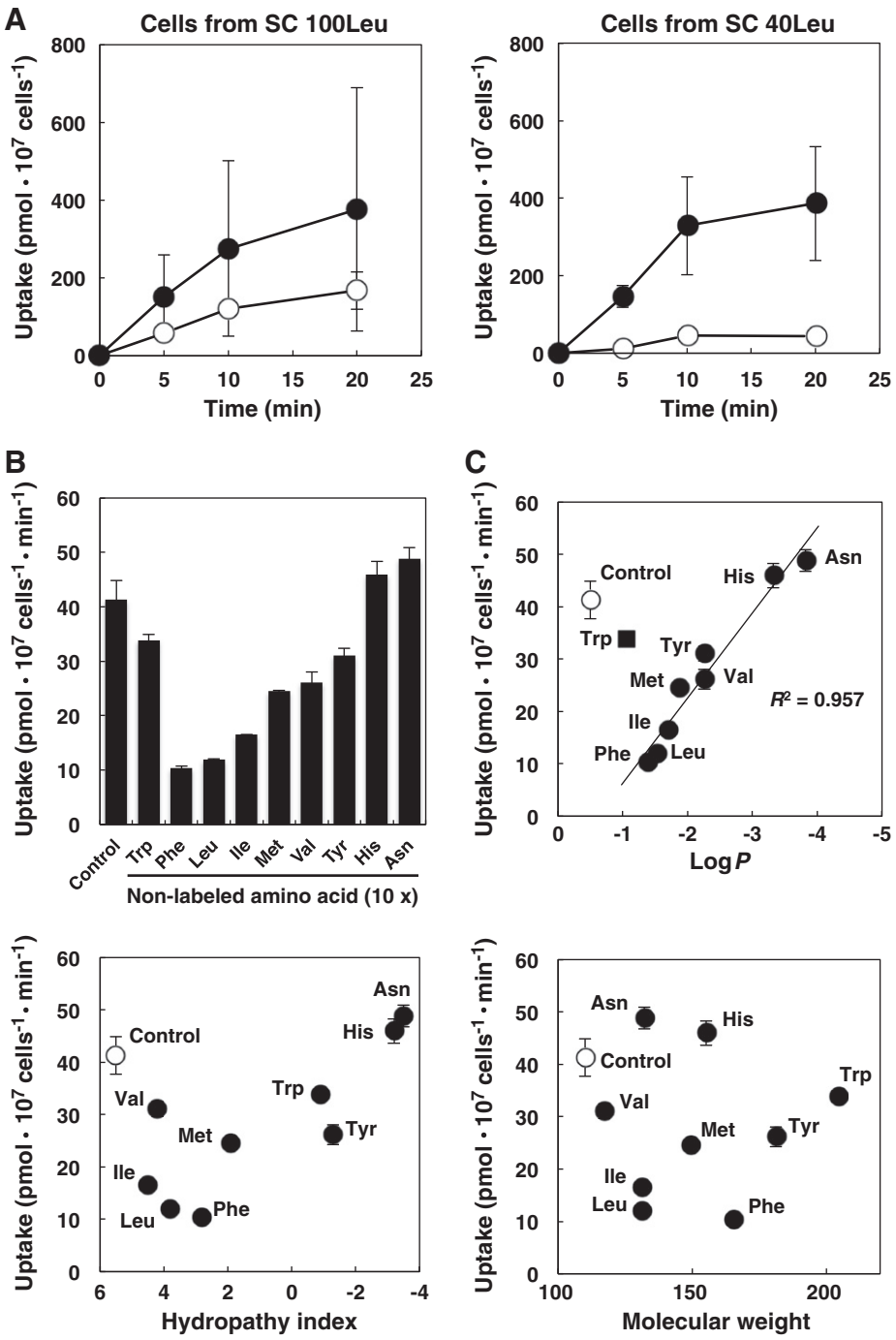

Fig. 6. Leucine uptake and import inhibition by amino acids. (A) Exponentially growing cells in SC 100Leu or SC 40Leu medium were subjected to an import assay in the presence of 4 μg·mL^{-1} (30.5 μM) of non-labeled leucine (see the Materials and methods section). (B) A leucine import assay was performed in the presence of 10-fold higher concentrations (305 μM) of non-labeled amino acids. (C) Inhibitory effects of the non-labeled amino acids versus log*P* values (octanol–water partition coefficient), hydropathy indices, and the molecular weights. Data are expressed as the mean values of incorporated leucine (pmol·10^7 cells^{-1} min^{-1}) with standard deviations obtained from three independent experiments.

import. The corresponding V168A mutation in Tat2 led to a more pronounced defect in tryptophan import, compared with tyrosine and phenylalanine import, in turn suggesting that V168 plays a partial role in the tryptophan selectivity of Tat2 [17]. Accordingly, C182 is unlikely to engage in leucine aliphatic side-chain recognition. In the modeled Bap2 structure, K242 (TMD5) faced I109 and G110, but the K242R mutation had no marked effect on leucine import. In contrast, the K228R mutation diminished tryptophan import by Tat2 [17]. Therefore, a positive charge at position 242 (K242 or R242) might be sufficient for Bap2, but lysine is required at position 228 in Tat2 and might possibly affect substrate recognition by the GTG motif. Amino acid residues in TMD7 have not been addressed in AdiC studies. Among the 5 mutations in TMD7 (Y336L, I341L, I343L, F345L, and V347L), only the Y336L mutation compromised leucine import. This is in sharp contrast to the significance of TMD7 in Tat2-mediated tryptophan import [17]. S393 (TMD8) and V394 (TMD8) are highly conserved in yeast amino acid permeases. In Gap1, S388 and V398 are exposed to the putative amino acid translocation pathway and are assumed to stimulate the PKA pathway upon nutrient addition to the cells [27]. However, in Bap2, V394 but not S393 was required for leucine import.

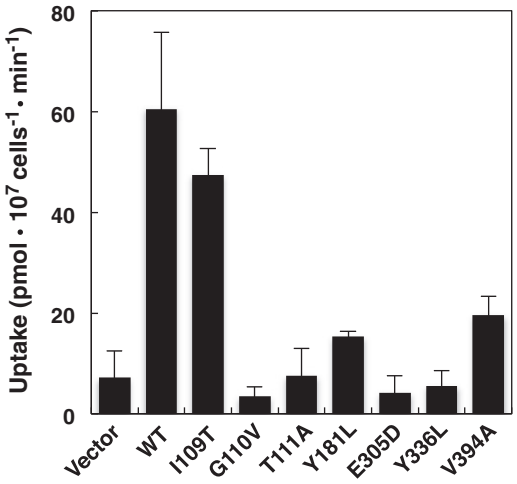

Fig. 7. Effects of Bap2 mutations on leucine import. Exponentially growing cells in SC 100Leu medium were shifted to SC 40Leu medium, followed by an additional 6-h incubation. Leucine uptake was measured as described in the Materials and methods section. Data are expressed as the mean values of incorporated leucine (pmol·10^7 cells^{-1} min^{-1}) with standard deviations obtained from three independent experiments.

4. Discussion

Among the yeast amino acid permeases with leucine-transport capability, we focused on the high-affinity leucine permease Bap2. Based on our prior observations with Tat2, we identified 7 amino acid residues required for leucine import in Bap2. Accordingly, Bap2 was more permissive to amino acid substitution than was Tat2 with respect to the critical sites confirmed in the Tat2 analysis. Further experiments are needed to verify whether these amino acid residues directly interact with leucine or indirectly affect substrate recognition or transport. In our previous study, we showed that tryptophan import was highly sensitive to high hydrostatic pressure [20], whereas leucine import was almost unaffected by pressure up to 50 MPa [30]. High pressure stiffens the lipid membranes [31], and thereby the TMD configurations of any membrane proteins are affected to some extent. The pronounced high-pressure sensitivity of Tat2 might be attributable to a delicate mechanism of tryptophan recognition and translocation, mediated by rigorous interactions between the substrate-binding site and the tryptophan side chain. In this light, the high-pressure resistance of Bap2 might agree with the fact that reduced numbers of amino acid residues were required for leucine import. The effects of hydrostatic pressure on an enzymatic reaction are interpreted by the simplest kinetic mechanism in which the transition state presents the highest energy barrier, and the chemical transformation of substrate to product is considered to be a single rate-limiting step [32,33]. Assuming that an amino acid is imported based on the simplest model, the differential effects of high pressure on Tat2 and Bap2 could also be attributable to the difference in conformational changes of the permease proteins associated with the substrate import; Tat2 undergoes a more pronounced conformational change than Bap2 does to form the transition-state ensemble. It is worthwhile elucidating whether any Bap2 mutations affect the high-pressure resistance of leucine import. Bap2-mediated high-affinity leucine import was inhibited by phenylalanine, leucine, isoleucine, methionine, tyrosine, valine, and tryptophan, which was consistent with the previous report in which *BAP2* overexpression enhanced the uptake of these amino acids [28]. One notable finding is that leucine import inhibition was clearly dependent on the log*P* values of the amino acids, except tryptophan. Hence, we proposed a working hypothesis

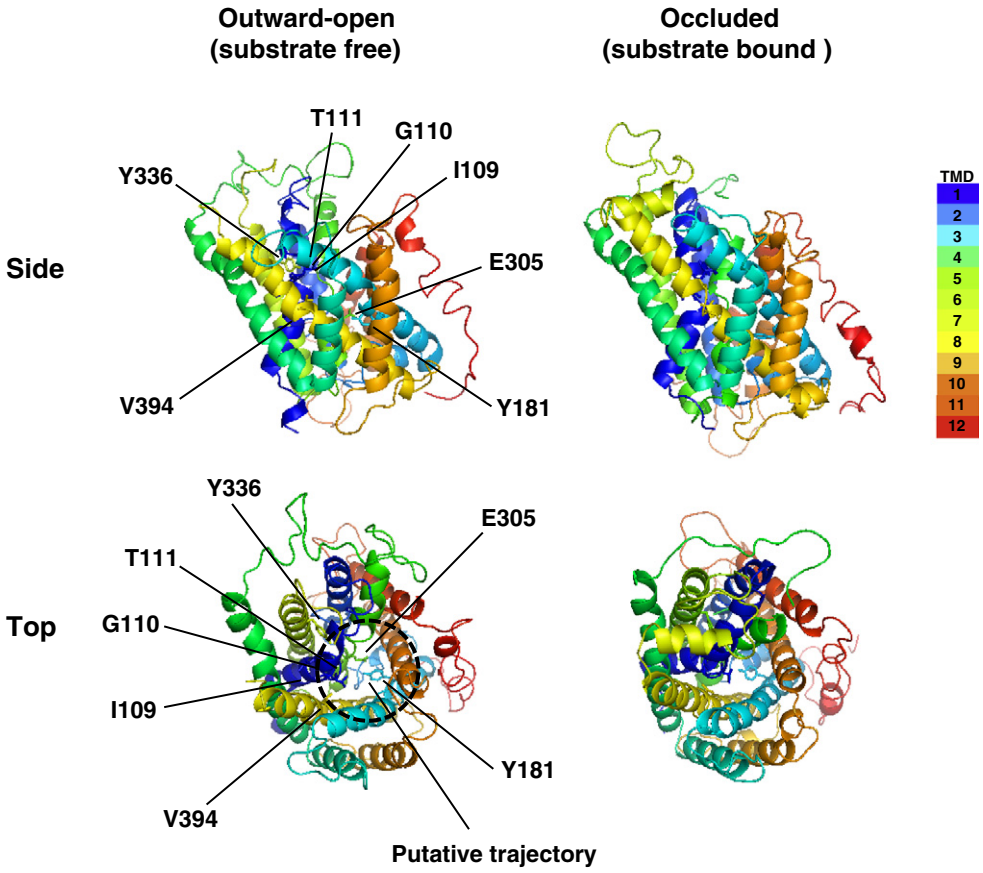

Fig. 8. Structural models of Bap2. Overall structures of Bap2 based on the AdiC outward-open (left, PDB: 3LRB as a template) [15] and occluded (right, PDB: 3L1L as a template) [16] crystal structures. Seven essential amino acid residues for leucine import are shown. The putative trajectory is circled.

that the log*P* value of a substrate would be the primary determinant of Bap2 selectivity, rather than the side-chain size or architecture alone. This might account for the broad substrate specificity observed for Bap2 in comparison to Tat2, which in turn suggests that Tat2 evolved as a distinct system to facilitate tryptophan uptake.

LeuT is a bacterial homologue of the neurotransmitter::sodium symporter family and has been successfully characterized by X-ray crystallography [34]. LeuT functions as a sodium-dependent symporter that is capable of transporting many hydrophobic amino acids, ranging from glycine to tyrosine. A requirement for a potential LeuT molecular substrate is that it must fit within the occluded substrate-binding cavity. Tryptophan is too large to be accommodated within this cavity and eventually becomes a non-transposable competitive inhibitor for LeuT. The LeuT–tryptophan complex adopts an open-to-out conformation because of the bulky size of tryptophan relative to the binding site. Singh et al. demonstrated that [^{3}H]-leucine binding to LeuT was inhibited by multiple aliphatic and aromatic amino acids of varying sizes in the following order of severity: leucine (−1.52) > methionine (−1.87) > alanine (−2.85) > tyrosine (−2.26) > tryptophan (−1.05) > glycine (−3.21; log*P* values are noted in parentheses) [35]. From their results, we noticed that the severity also roughly coincided with the log*P* values, except for tryptophan. In LeuT, the F259 and I359 side chains participate in van der Waals interactions with the leucine side chain. The I359Q mutation in LeuT was shown to convert the activity of tryptophan from an inhibitor to a transportable substrate, thus allowing the formation of the occluded state. The I359Q mutation introduces both steric and electrostatic changes in the LeuT binding site [35]. In rats, the L-type amino acid transporter 1 (LAT-1) is a Na^+-independent neutral amino acid transporter with broad specificity [36]. LAT-1-mediated phenylalanine import was strongly and competitively inhibited by aromatic amino acid derivatives such as L-dopa, α-methydopa, melphalan, triiodothyronine, and throxine, whereas phenylalanine methyl ester, *N*-methyl phenylalanine, dopamine, tyamine, carbidopa, and droxidopa did not inhibit phenylalanine import [37]. These inhibitory derivatives must contain free carboxyl and amino groups, and are also accompanied by a calculated log*P* value within a certain range (−0.1896 to 0.7654), with some exceptions. From this perspective, log*P* is a unique parameter that introduces the possibility of developing competitive inhibitors not only for yeast Bap2, but also for a broad range of amino acid permeases. To validate our hypothesis, we must determine the kinetic parameters for a series of amino acids in Bap2-mediated high-affinity leucine import.

The severity of the GTG motif mutations (I109T, G110V, and T111A) was inevitable, given the role of arginine carboxyl group recognition at the TMD1 helix-breaking region in AdiC. Near the Bap2 GTG motif, Y336 (TMD7) might donate π electrons to I109 for structural stabilization, as postulated for Tat2 (π–aliphatic chain interactions) [17]. This would account for the defective leucine import observed in the Y336L mutant. In the layer distal to the periplasm in AdiC, Y93 (TMD3), E208 (TMD6), and Y365 (TMD10) played a central role in arginine transport as the distal gate [16]. The hydrogen bond network surrounding E208 was thought to lock the 3 TMDs in a closed conformation, thus blocking substrate transport. Arginine binding is thought to disrupt interactions between E208 and Y93/Y365, thus causing additional changes in TMD3 and TMD10 to form the inward-open conformation of AdiC [16]. In this regard, the Y181L and E305D mutations are likely to compromise the conformational change in the TMDs upon leucine binding to Bap2.

E305 is highly conserved among yeast amino acid permeases and bacterial solute transporters, and hence this glutamate residue is assumed to play a central role across a broad substrate import range [17]. We proposed two working hypotheses in Tat2 suggesting that protonation/deprotonation of the E286 (E305 in Bap2) carboxyl group mediated proton influx coupled with tryptophan import [17], which is likely applicable to Bap2. First, the p*K*a of glutamate is approximately 4.07 in water, and hence the majority of the carboxyl group will be deprotonated at a neutral pH. Because proton extrusion by the plasma membrane H^+-ATPase Pma1 occurs to a great extent, the juxtamembrane extracellular region might become more acidic than the growth medium (pH 5–6). If the juxtamembrane pH is much less than 4, the E305 carboxyl chain of Bap2 could be protonated in the outward-open structure. Upon leucine binding, Bap2 would undergo a structural change to form the inward-open structure, and concomitantly protons would be released to the cytoplasm. Second, E305 is buried in the middle of the TMD6 helix, where the ambient dielectric constant (D) becomes much lower than that of water (D_{water}, approximately 80). Hence, the p*K*a of the E305 carboxyl group becomes much higher than 4.07 and thereby the carboxyl group can be loaded with a proton, even at a neutral pH [17]. The hypothetically high p*K*a value of E305 in a low dielectric membrane environment is in accordance with a recent report stating that p*K*a values of the glutamate residues buried within a staphylococcal nuclease protein were high (range, 5.2–9.4 and average, 7.7) [38]. In very large-scale studies, protonation of the *E. coli* lactose permease LacY was shown to precede sugar binding at a physiological pH and to exhibit a remarkably high p*K*a (approximately 10.5) for sugar binding [39]. In LacY, multiple amino acid residues, including Y236 (TMD7), E269 (TMD8), R302 (TMD4), H322 (TMD10), and E325 (TMD10), play central roles in proton translocation, but any single residue is unlikely to be responsible for the unique pH dependence of sugar binding [39]. These residues are located in the *C*-terminal 6-helix bundle and positioned in the approximate middle of the LacY molecule across from the sugar-binding site. Likewise, multiple amino acid residues located near E305 might also be involved in proton translocation through Bap2.

Acknowledgements

We thank Riseko Watanabe for technical assistance and Akio Kihara for providing plasmids. This work was supported by grants from the Japan Society for the Promotion of Science (No. 22658031 and No. 24580122 to F. Abe) and the Program for the Strategic Research Foundation at Private Universities by the Ministry of Education, Culture, Sports, Science, and Technology (No. 2013–2017).

References

[1] D.K. Layman, D.A. Walker, Potential importance of leucine in treatment of obesity and the metabolic syndrome, J. Nutr. 136 (2006) 319S–323S.
[2] M. Grenson, C. Hou, M. Crabeel, Multiplicity of the amino acid permeases in *Saccharomyces cerevisiae*. IV. Evidence for a general amino acid permease, J. Bacteriol. 103 (1970) 770–777.
[3] M. Grauslund, T. Didion, M.C. Kielland-Brandt, H.A. Andersen, *BAP2*, a gene encoding a permease for branched-chain amino acids in *Saccharomyces cerevisiae*, Biochim. Biophys. Acta 1269 (1995) 275–280.
[4] M. De Boer, J.P. Bebelman, P.M. Goncalves, J. Maat, H. Van Heerikhuizen, R.J. Planta, Regulation of expression of the amino acid transporter gene *BAP3* in *Saccharomyces cerevisiae*, Mol. Microbiol. 30 (1998) 603–613.
[5] A. Schmidt, M.N. Hall, A. Koller, Two FK506 resistance-conferring genes in *Saccharomyces cerevisiae*, *TAT1* and *TAT2*, encode amino acid permeases mediating tyrosine and tryptophan uptake, Mol. Cell. Biol. 14 (1994) 6597–6606.
[6] J.L. Schreve, J.K. Sin, J.M. Garrett, The *Saccharomyces cerevisiae YCC5* (YCL025c) gene encodes an amino acid permease, Agp1, which transports asparagine and glutamine, J. Bacteriol. 180 (1998) 2556–2559.
[7] X. Zhu, J. Garrett, J. Schreve, T. Michaeli, *GNP1*, the high-affinity glutamine permease of *S. cerevisiae*, Curr. Genet. 30 (1996) 107–114.
[8] C. Hein, J.Y. Springael, C. Volland, R. Haguenauer-Tsapis, B. Andre, *Npl1*, an essential yeast gene involved in induced degradation of Gap1 and Fur4 permeases, encodes the Rsp5 ubiquitin-protein ligase, Mol. Microbiol. 18 (1995) 77–87.
[9] K.H. Wolfe, D.C. Shields, Molecular evidence for an ancient duplication of the entire yeast genome, Nature 387 (1997) 708–713.
[10] T. Didion, B. Regenberg, M.U. Jorgensen, M.C. Kielland-Brandt, H.A. Andersen, The permease homologue Ssy1p controls the expression of amino acid and peptide transporter genes in *Saccharomyces cerevisiae*, Mol. Microbiol. 27 (1998) 643–650.
[11] F. Omura, Y. Kodama, T. Ashikari, The N-terminal domain of the yeast permease Bap2p plays a role in its degradation, Biochem. Biophys. Res. Commun. 287 (2001) 1045–1050.
[12] F. Omura, Y. Kodama, The N-terminal domain of yeast Bap2 permease is phosphorylated dependently on the Npr1 kinase in response to starvation, FEMS Microbiol. Lett. 230 (2004) 227–234.
[13] R. Cohen, D. Engelberg, Commonly used *Saccharomyces cerevisiae* strains (e.g. BY4741, W303) are growth sensitive on synthetic complete medium due to poor leucine uptake, FEMS Microbiol. Lett. 273 (2007) 239–243.

[14] J. Ding, J. Bierma, M.R. Smith, E. Poliner, C. Wolfe, A.N. Hadduck, S. Zara, M. Jirikovic, K. van Zee, M.H. Penner, J. Patton-Vogt, A.T. Bakalinsky, Acetic acid inhibits nutrient uptake in *Saccharomyces cerevisiae*: auxotrophy confounds the use of yeast deletion libraries for strain improvement, Appl. Microbiol. Biotechnol. 97 (2013) 7405–7416.
[15] X. Gao, F. Lu, L. Zhou, S. Dang, L. Sun, X. Li, J. Wang, Y. Shi, Structure and mechanism of an amino acid antiporter, Science 324 (2009) 1565–1568.
[16] X. Gao, L. Zhou, X. Jiao, F. Lu, C. Yan, X. Zeng, J. Wang, Y. Shi, Mechanism of substrate recognition and transport by an amino acid antiporter, Nature 463 (2010) 828–832.
[17] N. Kanda, F. Abe, Structural and functional implications of the yeast high-affinity tryptophan permease Tat2, Biochemistry 52 (2013) 4296–4307.
[18] G. Giaever, A.M. Chu, L. Ni, C. Connelly, L. Riles, S. Veronneau, S. Dow, A. Lucau-Danila, K. Anderson, B. Andre, A.P. Arkin, A. Astromoff, M. El-Bakkoury, R. Bangham, R. Benito, S. Brachat, S. Campanaro, M. Curtiss, K. Davis, A. Deutschbauer, K.D. Entian, P. Flaherty, F. Foury, D.J. Garfinkel, M. Gerstein, D. Gotte, U. Guldener, J.H. Hegemann, S. Hempel, Z. Herman, D.F. Jaramillo, D.E. Kelly, S.L. Kelly, P. Kotter, D. LaBonte, D.C. Lamb, N. Lan, H. Liang, H. Liao, L. Liu, C. Luo, M. Lussier, R. Mao, P. Menard, S.L. Ooi, J.L. Revuelta, C.J. Roberts, M. Rose, P. Ross-Macdonald, B. Scherens, G. Schimmack, B. Shafer, D.D. Shoemaker, S. Sookhai-Mahadeo, R.K. Storms, J.N. Strathern, G. Valle, M. Voet, G. Volckaert, C.Y. Wang, T.R. Ward, J. Wilhelmy, E.A. Winzeler, Y. Yang, G. Yen, E. Youngman, K. Yu, H. Bussey, J.D. Boeke, M. Snyder, P. Philippsen, R.W. Davis, M. Johnston, Functional profiling of the *Saccharomyces cerevisiae* genome, Nature 418 (2002) 387–391.
[19] R.S. Sikorski, P. Hieter, A system of shuttle vectors and yeast host strains designed for efficient manipulation of DNA in *Saccharomyces cerevisiae*, Genetics 122 (1989) 19–27.
[20] F. Abe, H. Iida, Pressure-induced differential regulation of the two tryptophan permeases Tat1 and Tat2 by ubiquitin ligase Rsp5 and its binding proteins, Bul1 and Bul2, Mol. Cell. Biol. 23 (2003) 7566–7584.
[21] J. Heitman, A. Koller, J. Kunz, R. Henriquez, A. Schmidt, N.R. Movva, M.N. Hall, The immunosuppressant FK506 inhibits amino acid import in *Saccharomyces cerevisiae*, Mol. Cell. Biol. 13 (1993) 5010–5019.
[22] A. Sali, T.L. Blundell, Comparative protein modelling by satisfaction of spatial restraints, J. Mol. Biol. 234 (1993) 779–815.
[23] C. Lambert, N. Leonard, X. De Bolle, E. Depiereux, ESyPred3D: prediction of proteins 3D structures, Bioinformatics 18 (2002) 1250–1256.
[24] W. DeLano, The PyMOL molecular graphics system, version 1.5.0.4 Schrödinger, LLC, (http://www.pymol.org/) The PyMOL User's Manual, San Carlos, CA, USA, DeLano Scientific, 2002.
[25] S.S. Nigavekar, J.F. Cannon, Characterization of genes that are synthetically lethal with *ade3* or *leu2* in *Saccharomyces cerevisiae*, Yeast 19 (2002) 115–122.
[26] V.A. Simossis, J. Heringa, PRALINE: a multiple sequence alignment toolbox that integrates homology-extended and secondary structure information, Nucleic Acids Res. 33 (2005) W289–W294.
[27] G. Van Zeebroeck, B.M. Bonini, M. Versele, J.M. Thevelein, Transport and signaling via the amino acid binding site of the yeast Gap1 amino acid transceptor, Nat. Chem. Biol. 5 (2009) 45–52.
[28] B. Regenberg, L. During-Olsen, M.C. Kielland-Brandt, S. Holmberg, Substrate specificity and gene expression of the amino-acid permeases in *Saccharomyces cerevisiae*, Curr. Genet. 36 (1999) 317–328.
[29] J. Kyte, R.F. Doolittle, A simple method for displaying the hydropathic character of a protein, J. Mol. Biol. 157 (1982) 105–132.
[30] F. Abe, Probing for dynamics of amino acid uptake in living yeast using hydrostatic pressure, in: F. Abe, A. Suzuki (Eds.), Proceedings for the 4th International Conference on High Pressure Bioscience and Biotechnology, J-STAGE, 1, 2007, pp. 134–138.
[31] R. Winter, W. Dzwolak, Exploring the temperature–pressure configurational landscape of biomolecules: from lipid membranes to proteins, Philos. Trans. A. Math. Phys. Eng. Sci. 363 (2005) 537–562 (discussion 562–563).
[32] K. Heremans, L. Smeller, Protein structure and dynamics at high pressure, Biochim. Biophys. Acta 1386 (1998) 353–370.
[33] C. Balny, P. Masson, K. Heremans, High pressure effects on biological macromolecules: from structural changes to alteration of cellular processes, Biochim. Biophys. Acta 1595 (2002) 3–10.
[34] S.K. Singh, C.L. Piscitelli, A. Yamashita, E. Gouaux, A competitive inhibitor traps LeuT in an open-to-out conformation, Science 322 (2008) 1655–1661.
[35] C.L. Piscitelli, E. Gouaux, Insights into transport mechanism from LeuT engineered to transport tryptophan, EMBO J. 31 (2012) 228–235.
[36] Y. Kanai, H. Segawa, K. Miyamoto, H. Uchino, E. Takeda, H. Endou, Expression cloning and characterization of a transporter for large neutral amino acids activated by the heavy chain of 4F2 antigen (CD98), J. Biol. Chem. 273 (1998) 23629–23632.
[37] H. Uchino, Y. Kanai, D.K. Kim, M.F. Wempe, A. Chairoungdua, E. Morimoto, M.W. Anders, H. Endou, Transport of amino acid-related compounds mediated by L-type amino acid transporter 1 (LAT1): insights into the mechanisms of substrate recognition, Mol. Pharmacol. 61 (2002) 729–737.
[38] D.G. Isom, C.A. Castaneda, B.R. Cannon, P.D. Velu, E.B. Garcia-Moreno, Charges in the hydrophobic interior of proteins, Proc. Natl. Acad. Sci. U. S. A. 107 (2010) 16096–16100.
[39] I.N. Smirnova, V. Kasho, H.R. Kaback, Protonation and sugar binding to LacY, Proc. Natl. Acad. Sci. U. S. A. 105 (2008) 8896–8901.